Original Article

Characterization of ore types in the Complexo Alegria (Mariana, Brazil): focus on phosphorous, aluminum and titanium contaminants

Ana Maria Guilherme Bailon [1]*
Leonardo Esteves Bonfioli [2]
Gil Ribeiro Vilela Neto [1]
Sandra Cristina da Silva Porto [1]
Daniel Avelar Lucena [1]
Luís Marcelo Tavares [3]

Abstract

One important aspect of the geometallurgical characterization of iron ore mining operations is to evaluate the content of chemical elements that are deleterious due to their impact on the quality of agglomerates and the performance of steel products. This study characterizes iron ore typologies focusing on the presence of phosphorus, aluminum, titanium and LOI in ores in order to support studies on phosphorus removal. Samples of mining faces from the Alegria Complex (Minas Gerais, Brazil) from typologies that were rich in aluminum were selected in particular owing to their detrimental impact on the floatability of the ores. In addition, mineralogical, chemical, particle size and microstructural analyses were carried out on samples of iron ore and tailings. The studies identified levels of deleterious elements in the concentrate and flotation tailings and slimes, associating them with typologies and mining faces, as well as their forms of occurrence in the ore, providing important insights for studies that aim to remove contaminants in Samarco´s products.

Keywords: Geometallurgy; Typology; Phosphorus; Aluminum; Titanium.

1 Introduction

It has become evident that, as exploitation evolves, iron ore deposits from the *Quadrilátero Ferrífero* province have average grades dropping, with an increase in the proportion of gangue and deleterious components, namely, silica, alumina, phosphorus and titanium, besides the appearance of hydrated minerals [1]. This has demanded improvement in techniques used in mining and processing of these ores. Samarco Mineração S.A. has been engaged in geometallurgical studies of its mineral deposits with the aim of improving the quality of concentrates from its plants at Germano (Minas Gerais, Brazil), besides its industrial pelletization complex at Ubu (Espírito Santo, Brazil).

As part of the geometallurgical characterization it is important to understand about the geological formation of the processed ores. Indeed, hypergenic metasomatic deposits were products of tectonic and metamorphic processes that acted on the iron ores generating either itabirites or hematite-rich rocks called hematitites. These deposits are characterized by replacement of quartz in the iron ores by hot hydrothermal fluids that originated from great depths. On the other hand, supergene enrichment is result of weathering the iron ores with replacement of quartz and other minerals by iron brought from colder solutions from the surface, mostly associated with rainfall [1]. In the case of the Alegria Complex (Minas Gerais), iron ores were mostly generated as result of supergene enrichment, being common the presence of high goethite contents, which is a key carrier of contaminants [1].

The so-called gangue minerals in itabirite iron ores, typically containing silica, alumina and phosphorus, have deleterious impacts on iron production. In particular, well-known gangue minerals in itabirite iron ores include quartz (SiO_2), gibbsite ($Al(OH)_3$), kaolinite ($Al_2Si_2O_5(OH)_4$), besides minerals from the amphibole group [2]. Gangue minerals may be discarded as part of mineral processing operations that are able to reduce their concentration. In the case of flotation, aluminum has been known to reduce the ability of the gangue minerals to adhere to the air bubbles in the reverse flotation scheme [2]. This results in impacts on separation of valuable minerals such as hematite, which may report to the froth product along with the gangue minerals, reducing the iron content of the concentrate produced.

---

[1] *Samarco Mineração, Anchieta, ES, Brasil.*
[2] *Samarco Mineração, Germano, MG, Brasil.*
[3] *Laboratório de Tecnologia Mineral, Instituto Alberto Luiz Coimbra de Pós-graduação e Pesquisa de Engenharia – COPPE, Universidade Federal do Rio de Janeiro – UFRJ, Rio de Janeiro, RJ, Brasil.*

**Corresponding author: anamag@samarco.com*
E-mails: bonfioli@samarco.com; gil.ribeiro@samarco.com; sandrap@samarco.com; daniel.avelar@samarco.com; tavares@metalmat.ufrj.br

If alumina-containing components are not removed from the iron ore, then the resulting steel may exhibit lower ductility and become brittle. In the process of fusion, the high aluminum content is known to interfere with the slag viscosity, impacting the control of metallurgical variables [3]. Phosphorus, when present in high contents in steels, can also result in their embrittlement [3], thus limiting exploitation of ores from deposits rich in them, in particular in the case of those rich in ores from either weathered or supergenic origin. The identification of minerals containing phosphorus is often a challenge, which often makes their removal inefficient.

Previous studies on mineralogical characterization of phosphorus contained in iron ores identified various forms of its occurrence [1]. Electron microprobe studies suggested that phosphorus may be associated with goethite, located within discrete inclusions of very fine sizes. These associations are very particular and are a function of several factors, which include location within the mineral deposit, origin, mineralogy, etc, with no general pattern having yet been identified [1].

Studies have shown that interaction of phosphate and goethite involve ternary adsorption and superficial precipitation [4]. These have been proposed to include the dissolution of goethite crystals and subsequent adsorption of iron associated with phosphate [1]. The surface of precipitation of anions involved in the model includes the dissolution of goethite that introduces the iron cations in the crystalline structure. The proposed process includes four distinct stages. The first consists in the arrival of phosphate in either mono or bi-dented with hydroxyls on the surface of goethite. In the second stage, after adsorption, phosphate acts as sorption sites for dissolved iron, forming a ternary complex that reduces iron concentration in the solution. In the third stage, goethite is dissolved, releasing the iron ions to the solution, which in turn adsorbs phosphate in its surface. The adsorbed anions may form ternary complexes with metals in solution. In the last stage the adsorbed iron offers sorption sites for phosphate and the process continues. In steel production phosphorus dissolves within ferrite, hardening it and resulting in cold embrittlement of the steel, resulting in low impact resistance and low toughness. Besides that, phosphorus is one of the elements that are responsible for embrittlement after tempering.

Owing to these factors, the maximum content of phosphorus in the concentrate is strictly controlled in steels within the range 0.005 and 0.1%, varying depending on the desired quality and application of steel [1].

The present work aims to map the alumina-rich ores present in different mining faces of the Alegria deposit, with the final goal of identifying the forms of occurrence of phosphorus and aluminum in the ores from the deposit, owing to the potential impact on the final quality of the iron ore pellets produced. This focus on alumina-rich ores is owing to their detrimental impact on floatability of the ores. On the other hand, although not typically listed as a deleterious component, this work also analyzes the presence of titanium, owing to its association with goethite and aluminum components with direct impacts on flotation performance.

2 Materials and methods

Iron ore samples from 23 different mine faces from the Alegria Norte e Sul mining complex, located in the *Quadrilátero Ferrífero* de Minas Gerais (Brazil), were collected. Each of the mining faces represents a different mining block at the site. In this block model, information regarding geology, mineralogy, chemical composition, metallurgical and geotechnical parameters are mapped.

Each sample, containing approximately 30 kg, was initially subdivided for analyses and testing by coning and quartering. Chemical analyzes were carried out by X-ray fluorescence spectrometry [5] in a Rigaku Simultaneous Multi-Element wavelength dispersive X-Ray Fluorescence (WDXRF) Spectrometer Simultix 14, in which fused samples were analyzed using standard references. These have been complemented with loss on ignition (LOI) by the gravimetric method [6], elemental carbon and sulfur analysis in a LECO-CS analyzer and total iron measurement by the titration method [7]. Mineralogical analyzes were carried out using the Imager M.2m optical microscope, equipped with motorized table and a camera. Analyzes were carried out with the support of the image analysis software called Zencore. In addition, scanning electron microscopy (SEM) model FlexSEM 1000II by Hitachi, equipped with energy-dispersive spectroscopy (EDS), was used to identify the elemental composition of the samples. In addition, mineralogical quantifications were also carried out in SEM using the AMICS system.

After the preliminary analysis, the 23 samples were grouped in pairs with similar mineralogy, independently of either iron or contaminant contents. The sample with high magnetite content was identified but was not analyzed in greater detail given the low proportion of this mineral in the Alegria deposit. The samples were then subjected to the processes of grinding, classification, desliming and flotation at pilot-scale until they reached the typical iron content in the concentrate at Samarco, required for production of direct reduction pellets. The samples from the grinding stage were subjected to wet sieving, besides detailed liberation analyzes. The concentrate, sandy tailings and slimes generated in the process were analyzed aiming to map the concentration of contaminants in the various products.

3 Results and discussion

First, the results from chemical (X-ray fluorescence) and mineralogical analyzes (optical microscopy) of the concentrate, slimes and tailings are presented in Figure 1. They show that the flotation concentrate is composed of different iron oxides, which carry substantial proportions of

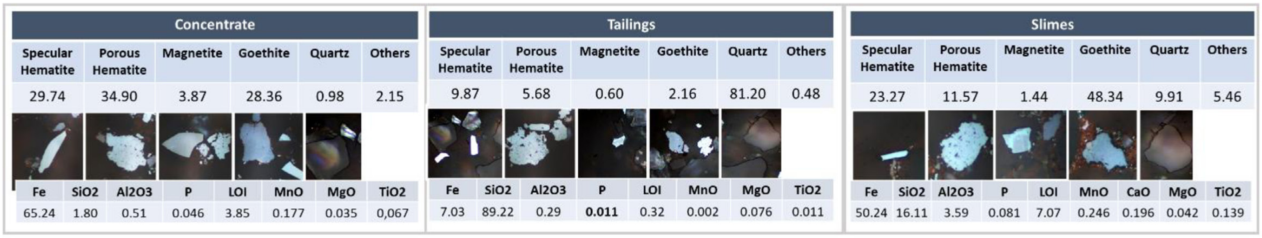

Concentrate

Specular Hematite	Porous Hematite	Magnetite	Goethite	Quartz	Others
29.74	34.90	3.87	28.36	0.98	2.15

Fe	SiO2	Al2O3	P	LOI	MnO	MgO	TiO2
65.24	1.80	0.51	0.046	3.85	0.177	0.035	0,067

Tailings

Specular Hematite	Porous Hematite	Magnetite	Goethite	Quartz	Others
9.87	5.68	0.60	2.16	81.20	0.48

Fe	SiO2	Al2O3	P	LOI	MnO	MgO	TiO2
7.03	89.22	0.29	**0.011**	0.32	0.002	0.076	0.011

Slimes

Specular Hematite	Porous Hematite	Magnetite	Goethite	Quartz	Others
23.27	11.57	1.44	48.34	9.91	5.46

Fe	SiO2	Al2O3	P	LOI	MnO	CaO	MgO	TiO2
50.24	16.11	3.59	0.081	7.07	0.246	0.196	0.042	0.139

Figure 1. Results from mineralogical and chemical analyzes of iron ore concentrate, tailings and slimes and micrographs of the different minerals identified.

contaminants, including phosphorous, alumina and silica. The micrographs illustrate that the same minerals appear in the tailings and slimes, although in different concentrations**.** A substantial part of goethite, phosphorous and alumina is present in the slimes. A high content of specular hematite is also present in the slimes. This is the mineral of greatest interest to report to the concentrate stream, so that losses in the tailings are associated with its high content in the feed.

From this point onwards, all analyzes are related to the mine face samples. A summary of the mineralogical analyses results from optical microscopy is presented in Figure 2, which shows relevant differences in the goethite, porous hematite (martite) and specular (compact) hematite contents among the mining faces. The column identified as "others", which contains clay minerals as well as other iron-containing minerals, also varied significantly. Also in Figure 2 are the results from analysis of the phosphorous (X-ray fluorescence) and iron (titration), varying significantly among the mining faces.

The figure shows that the mine faces that contain the highest contents of goethite and phosphorus were also those with the highest iron contents (Fe_T), demonstrating the challenge in defining the blend of ores that should feed the concentration and then the pelletization plants, with acceptable phosphorus contents. A summary of the chemical analysis of the samples from the different faces is summarized in Table 1. It shows that some samples present higher iron content and LOI, whereas other higher contamination by phosphorus and alumina, whereas yet others with higher manganese and titanium contents. In the geometallurgical modeling of the Alegria mine complex, the most important contents are those of iron, phosphorus and LOI.

The samples, now grouped into 12 new samples following their mineralogical characteristics (section 2), are then further analyzed as follows. A summary of size analyses of the ground samples is presented in Figure 3. It shows that, after grinding, the different mine faces present reasonable variations in size distribution, with a highlight to AGEO-145-4, which likely presents lower grindability. These differences probably impacted liberation and concentration response of the samples.

Results from liberation analyzes are summarized in Table 2. It shows that the goethite and the iron-oxide phases (OxFe) are strongly associated with each other. This has significant implications for liberation, and, therefore, separation of the phases during mineral processing. Indeed, results are presented in Table 2 considering the separation of the binary system, namely quartz from the combination of iron oxides and goethite. The Gaudin method [8] considers that the class which has exposure higher than 90% are regarded as liberated. As such, Table 2 summarizes the results for the proportions of liberated grains (>90%) composed either by a combination of iron oxides and goethite or quartz.

Figure 4 shows the variation of cumulative liberation as a function of liberation class. On the basis of the cumulative liberation of the iron oxide phases, it is evident that the iron minerals in several of the samples (AGEO-142-8, AGEO-145-4, AGEO-152-2, AGEO-153-3, AGEO-156-6 and AGEO-158-8) exhibit good liberation, with values higher than 94.7%. On the other hand, two of the samples, namely AGEO-137-3 and AGEO-138-4, present only 78.0% and 80.3% of particles liberated containing iron oxides, respectively.

Also, from the cumulative liberation pattern, it is evident that quartz exhibits good liberation in the samples AGEO-143-2, AGEO-152-2, AGEO-156-6 and AGEO-158-8, with values exceeding 90%, whereas samples AGEO-137-3, AGEO-138-4, AGEO-145-4 and AGEO-154-4 present less than or 78% liberation, namely 64.2%, 72.3%, 78.0% and 61.9% of the liberated particles, respectively, with values in between for the remaining samples.

As such, with the exception of samples AGEO-143-2 and AGEO-157-7, iron minerals present greater liberation than quartz. Two of the samples, those presenting the highest goethite, phosphorus and iron contents, were additionally subjected to analysis of mineral associations, namely, the type of minerals and quantification of the amounts of particles composed of either one, two or three phases. This analysis is associated with the degree of liberation of iron-containing minerals and to the presence of contaminants in the concentrate since, even after comminution and concentration, some associations of the valuable minerals with the contaminants persist, in particular with silica, aluminum, phosphorus and, in smaller degree, kaolinite. Figure 5 shows the classification of particles and the associations identified for sample AGEO-152-2, showing that 17% are represented by a single phase, 77% are binary and 6% are ternary. In this assessment it is evident the high degree of association of the particles and the fact that even phosphates are associated with iron oxides.

The mineral associations and the presence of clay minerals in the ore samples have been investigated, with a

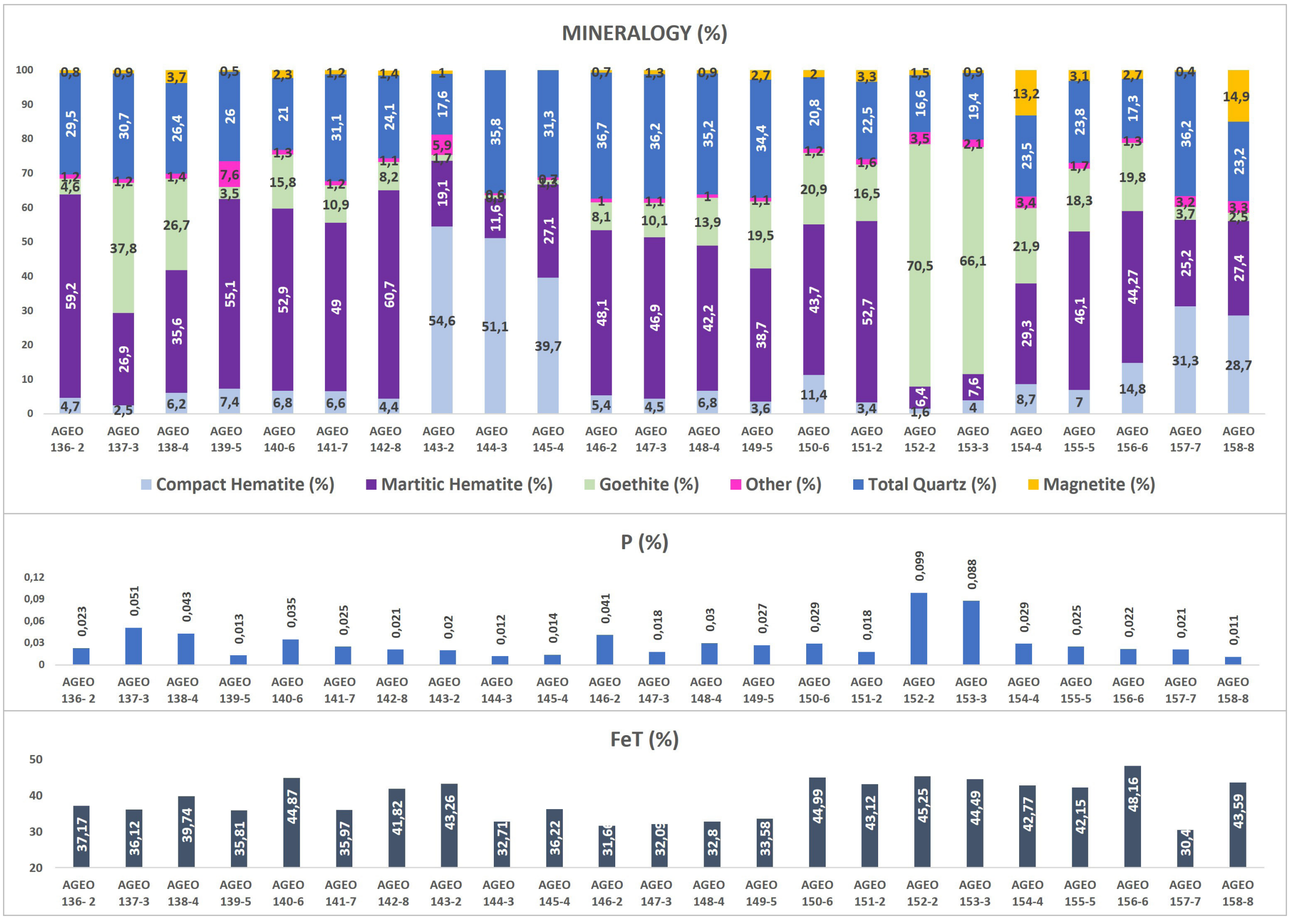

Figure 2. Summary of characterization results from the different mine face samples.

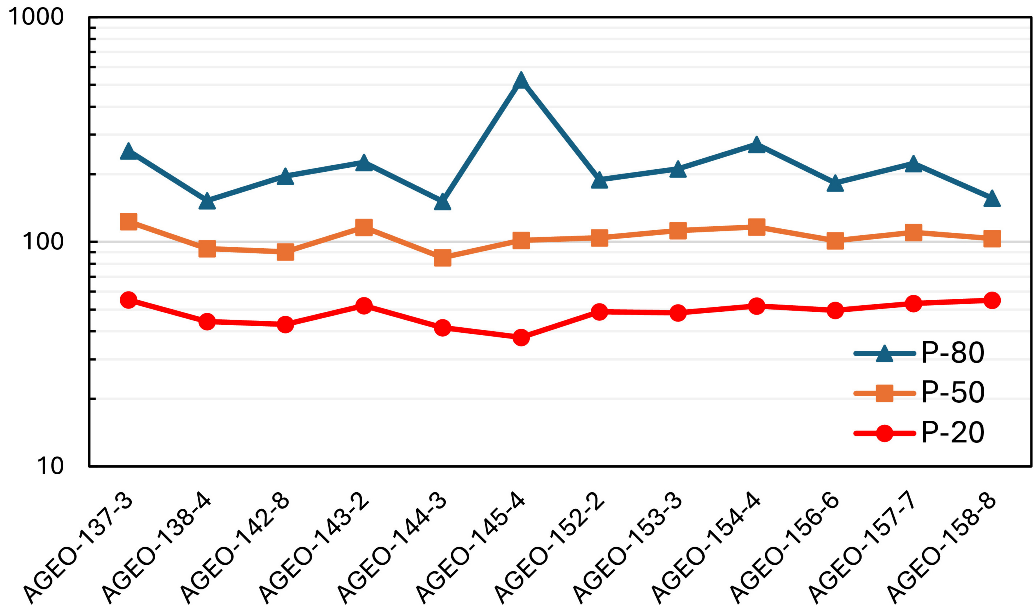

Figure 3. 80, 50 and 20% passing sizes of selected samples (in μm).

Table 1. Summary of the chemical analysis results of the mine face samples by XRF, gravimetry and elemental analyses

	AGEO - 136- 2	AGEO - 137-3	AGEO - 138-4	AGEO - 139-5	AGEO - 140-6	AGEO - 141-7	AGEO - 142-8	AGEO - 143-2	AGEO - 144-3	AGEO - 145-4	AGEO - 146-2	AGEO - 147-3	AGEO - 148-4	AGEO - 149-5	AGEO - 150-6	AGEO - 151-2	AGEO - 152-2	AGEO - 153-3	AGEO - 154-4	AGEO - 155-5	AGEO - 156-6	AGEO - 157-7	AGEO - 158-8
FeT (%)	37.17	36.12	39.74	35.81	44.87	35.97	41.82	43.26	32.71	36.22	31.66	32.09	32.8	33.58	44.99	43.12	45.25	44.49	42.77	42.15	48.16	30.43	43.59
FeO (%)	0.27	0.21	0.64	0.27	0.83	0.36	0.29	0.21	0.21	0.25	0.21	0.3	0.22	0.45	0.67	0.8	0.47	0.5	3.01	1.08	0.82	0.21	3.12
SiO_2 (%)	44.82	44	39.7	47.38	33.41	46.28	37.99	29.07	52.38	47.23	52.71	51.98	50.69	49.36	32.88	35.37	24.9	28.77	36.06	36.87	28.24	52.08	36.82
Al_2O_3 (%)	0.86	0.23	0.2	0.49	0.16	0.64	0.73	5.7	0.36	0.46	0.49	0.5	0.43	0.15	0.18	0.59	1.2	0.25	0.2	0.22	0.24	2.55	0.55
CaO (%)	0.01	0.01	0.01	0.01	0.01	0.01	0.01	0.01	0.01	0.01	0.01	0.01	0.01	0.01	0.01	0.01	0.01	0.01	0.01	0.01	0.01	0.01	0.01
MgO (%)	0.02	0.02	0.03	0.02	0.02	0.02	0.02	0.04	0.02	0.02	0.03	0.02	0.02	0.03	0.02	0.03	0.03	0.02	0.03	0.02	0.02	0.06	0.17
P (%)	0.023	0.051	0.043	0.013	0.035	0.025	0.021	0.02	0.012	0.014	0.041	0.018	0.03	0.027	0.029	0.018	0.099	0.088	0.029	0.025	0.022	0.021	0.011
Mn (%)	0.013	0.003	0.011	0.005	0.012	0.005	0.001	0.004	0.001	0.001	0.001	0.001	0.001	0.001	0.01	0.008	0.168	0.657	0.015	0.113	0.026	0.001	0.029
TiO_2 (%)	0.03	0.001	0.001	0.01	0.002	0.011	0.022	0.67	0.043	0.022	0.041	0.01	0.009	0.001	0.002	0.014	0.067	0.003	0.001	0.001	0.001	0.331	0.007
LOI (%)	1	3.92	3.12	0.81	2.16	1.51	1.34	2.54	0.33	0.39	1.3	1.51	1.81	2.34	2.5	2.29	8.63	6.26	2.72	2.45	2.56	1.35	0.33
S (%)	0.001	0.002	0.002	0.001	<0.001	0.002	0.002	0.002	<0.001	<0.001	0.001	0.002	0.002	0.002	0.002	0.002	0.016	0.004	0.006	0.003	0.006	0.001	0.002
C (%)	0.011	0.032	0.013	0.011	0.016	0.013	0.011	0.012	0.01	0.007	0.009	0.012	0.014	0.02	0.019	0.013	0.123	0.047	0.032	0.017	0.021	0.013	0.01

Table 2. Percentage of released grains (particles liberated >90%) for the studied phases in the ground samples

Sample	OxFe+Goethite	Quartz
AGEO-137-3	78.0	64.2
AGEO-138-4	80.3	72.3
AGEO-142-8	94.7	85.9
AGEO-143-2	87.1	94.8
AGEO-144-3	89.4	87.0
AGEO-145-4	93.8	78.0
AGEO-152-2	98.1	89.8
AGEO-153-3	94.9	79.6
AGEO-154-4	85.4	61.9
AGEO-156-6	98.7	91.7
AGEO-157-7	86.8	88.6
AGEO-158-8	97.7	93.0

summary of results in Table 3. For instance, it demonstrated that the contaminant aluminum is carried by goethite, kaolinites, micas, feldspars and gibbsites. Phosphorus is carried mostly by goethite and phosphates, in particular apatite. Manganese is mostly carried by oxy-hydroxy manganese, with up to 5% participation of amphibolites. Titanium is mostly carried within ilmenite, titanium oxides, iron oxides, goethite and kaolinite. Previous studies [3,9,10] with the iron ore from the same Alegria mine have shown that the greatest association of phosphorus has been with goethite and limonite and that the contents of phosphorus, silica, aluminum and iron varied significantly within the samples studied. The authors suggested that clay minerals containing phosphorus either within their structure or their surface as submicron grains, would fill cracks and even pores.

Table 3. Mineral associations, in percentage in volume, of OxFe and Goethite for the different samples

Sample	AGEO-137-3	AGEO-138-4	AGEO-142-8	AGEO-143-2	AGEO-144-3	AGEO-145-4	AGEO-152-2	AGEO-153-3	AGEO-154-4	AGEO-156-6	AGEO-157-7	AGEO-158-8
Quartz	13.88	12.46	2.27	0.66	5.75	6	0.95	2.97	9.41	1.06	4.62	0.7
Feldspar	0	0	0	0	0	0	0	0	0	0	0	0
Mica	0.01	0	0	0.12	0.01	0.03	0	0	0	0	0.66	0
Kaolinite	0.04	0.35	1.15	12.94	0.16	0.6	0.43	0	0.15	0.21	3.93	0.17
Chlorite	0	0	0	0	0	0	0	0	0	0	0	0
Talc	0	0	0	0	0	0	0	0	0	0	0	0.02
Amphibole	0.01	0	0	0	0	0	0	0	0	0	0	0
OxFe	0	0	0	0	0	0	0	0	0	0	0	0
Gibbsite	0.07	0	0.02	0.1	0.07	0.12	0.14	0.09	0	0.01	0.03	0.02
Ilmenite	0	0	0.01	0.82	0	0	0.17	0	0	0	0.19	0
OxTi	0	0	0	0.15	0	0.02	0	0	0	0	0.09	0
OxMn	0	0	0	0	0	0	0.12	0.55	0.02	0	0	0
Carbonate	0.14	0.02	0.02	0.17	0.04	0.01	0	0	0	0.01	0	0.01
Phosphate	0	0	0	0	0	0	0	0	0	0	0	0.01
Others	0.01	0	0	0.01	0	0.08	0	0	0.01	0	0.04	0
Low_Counts	0	0	0	0	0.01	0	0	0	0	0.01	0.01	0.06
Shadows	0	0	0	0	0	0	0	0	0	0	0	0
Un_x_rayed	0	0	0	0	0	0	0	0	0	0	0	0
Unknown	0.01	0	0.02	0.01	0	0.02	0.01	0.01	0.02	0.02	0.02	0.01
Pores	13.06	3.07	10.2	8.42	10.08	17.97	11.27	12.76	7.67	5.88	6.7	12.42
Free Surface	72.76	84.09	86.32	76.59	83.86	75.16	86.91	83.61	82.72	92.78	83.71	86.56

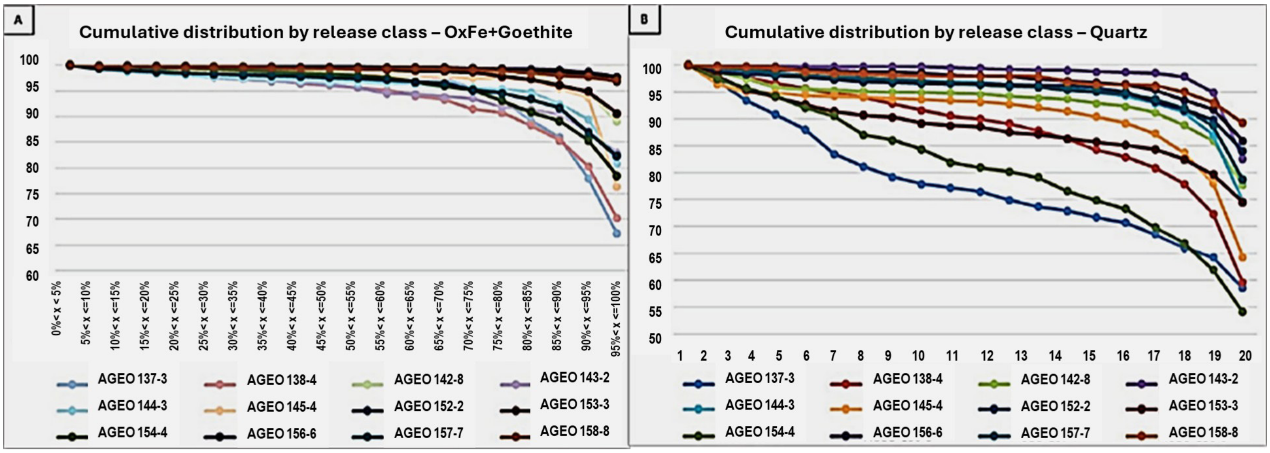

Figure 4. Cumulative liberation as a function of liberation class of the ground samples.

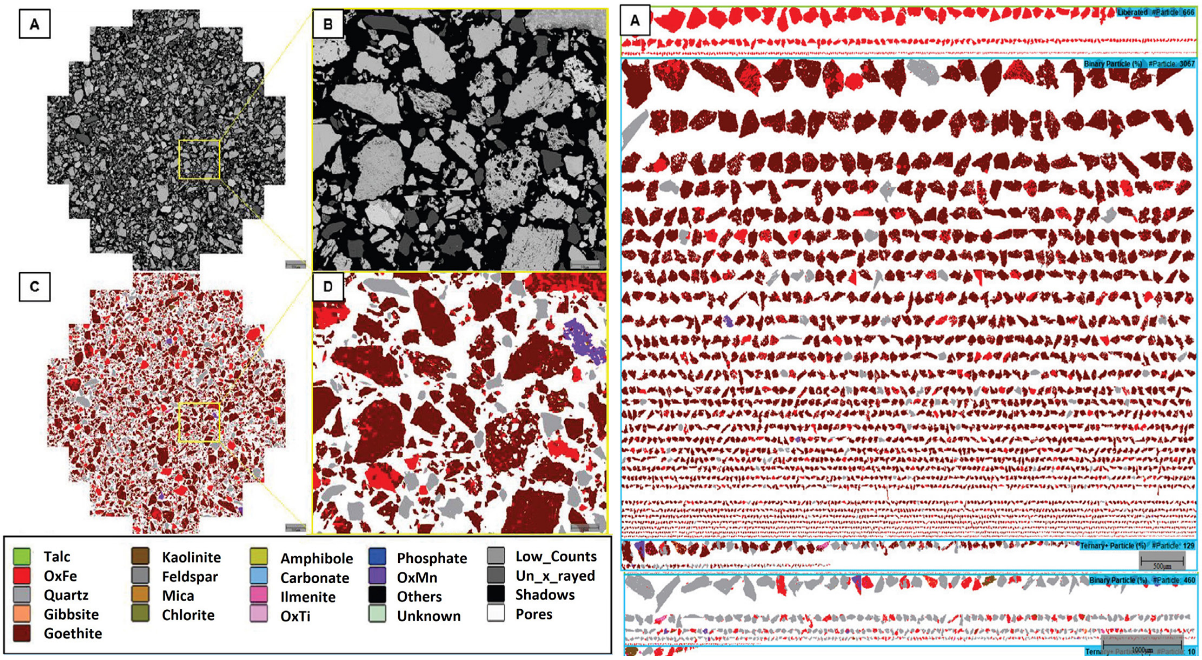

Figure 5. Classification of particles from SEM analysis of sample AGEO-152-2 after grinding.

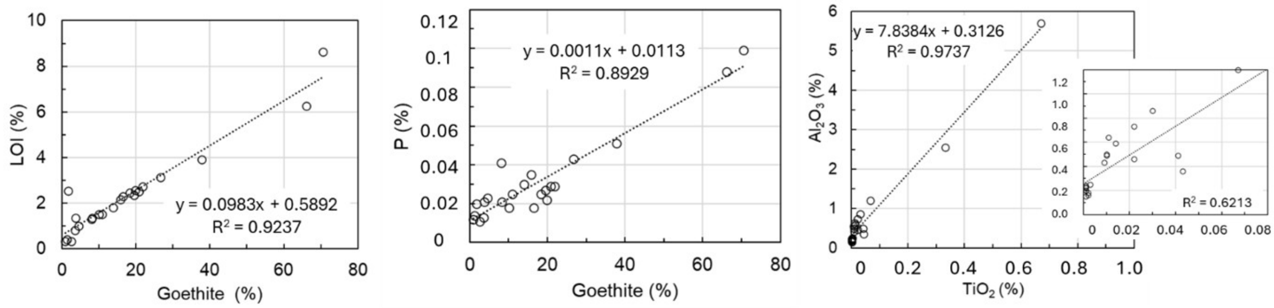

Figure 6. Correlations of selected components in the ore samples. The insert on the right presents the correlation for TiO_2 < 0.1%.

From the clay minerals identified, the mineral associations, the mineralogy and the chemical analyses, it is possible to establish a correlation between the goethite and LOI with the phosphorus content, with R^2 of 0.89 and 0.92, respectively (Figure 6). In analogy it has been possible to establish the relationship between alumina and titania contents, with R^2 of 0.97. Owing to the significant impact of the high titania values of a few samples, correlation has been further analyzed by removing data for TiO_2 < 0.1%, resulting in a good correlation between titania and alumina (R^2 = 0.62) (insert in Figure 5). The figure shows the relationships, indicating that the main source of phosphorus in the ore is goethite. However, goethite is not the only source of phosphorus in the ore. Also, the strong correlation between aluminum and titanium results in carry-over of titanium by mine faces that also have high aluminum contents.

In the analyzes under the microscope goethites that did carry phosphorus in their structure were also identified, demonstrating the coefficient of correlation below 1 (0.89 in Figure 5) beweeen goethite and phosphorus content. Indeed, Figure 7 shows a compact goethite particle which does not contain phosphorus, but contains silica in its structure.

Previous studies [9] have shown that phosphorus appears also as primary material in phosphorites (apatite and frankolite) in association to iron minerals. In supergenic ores, phosphorus may also appear in solid solutions in goethite associated with secondary minerals carrying iron and aluminum. Figure 8 shows a kaolinite particle containing phosphorus in its structure.

Figure 9 shows yet another source of phosphorus in the iron ore. Gibbsite can present phosphorus in its structure. The presence of calcium and titanium in the

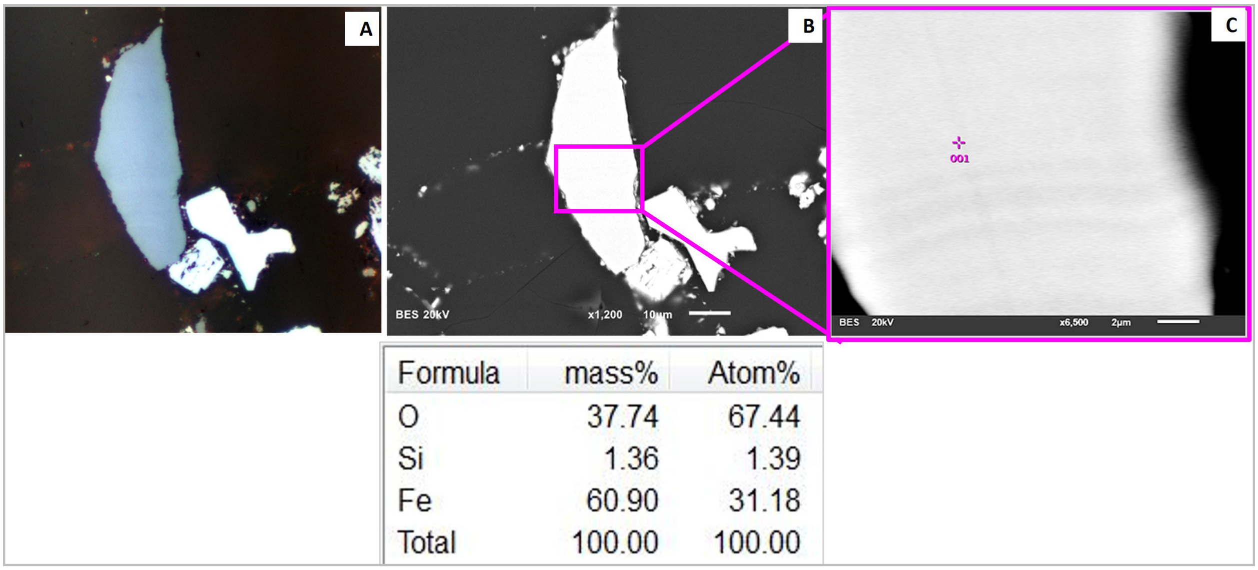

Formula	mass%	Atom%
O	37.74	67.44
Si	1.36	1.39
Fe	60.90	31.18
Total	100.00	100.00

Figure 7. Micrographs of massive goethite by optical microscopy (A) and SEM (B and C) and microprobe analyzes (below).

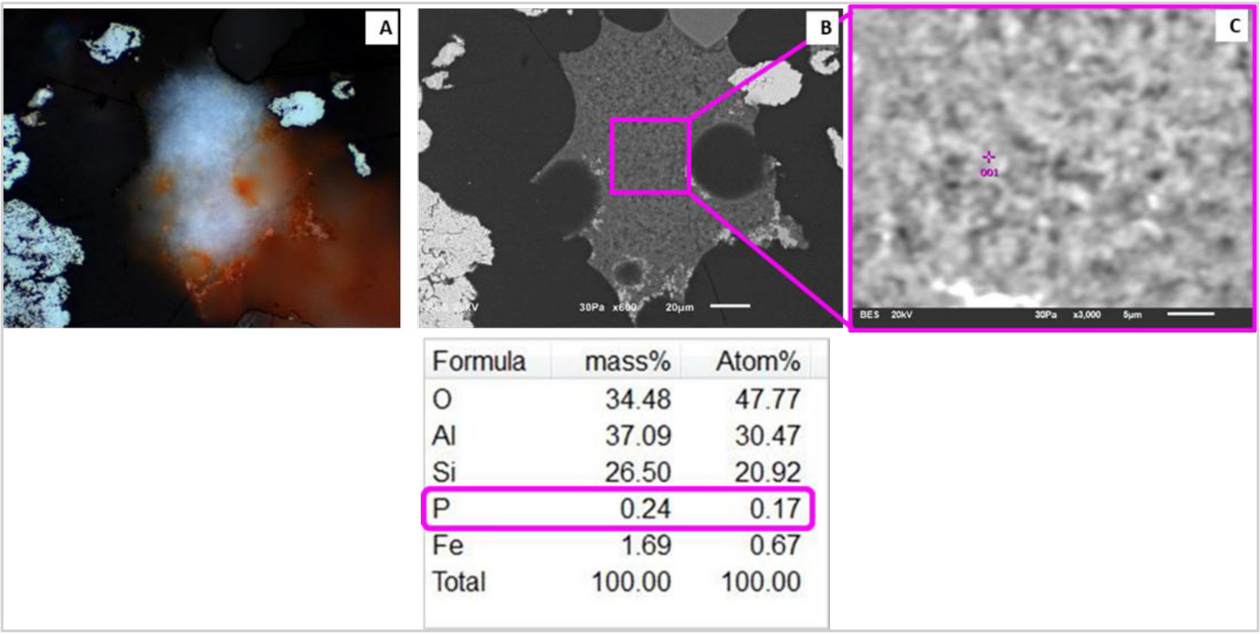

Formula	mass%	Atom%
O	34.48	47.77
Al	37.09	30.47
Si	26.50	20.92
P	0.24	0.17
Fe	1.69	0.67
Total	100.00	100.00

Figure 8. Micrographs of kaolinite containing phosphorus in its structure by optical microscopy (A) and SEM (B and C), and microprobe analyzes (below).

particle in question further supports the strong correlation between aluminum and titanium.

Kaolinite is a phyllosilicate with chemical formula given by $Al_2Si_2O_5(OH)_4$. If present in larger quantities, it may be the main source of silica and alumina. Indeed, studies of flotability of ores as a function of time [11] demonstrated that the flotation kinetics of kaolinite is substantially slower than that of quartz, concluding that in order to float kaolinite in industrial flotation plants the residence time in the cell should be very high, resulting in challenges in flotation of hematite, resulting in loss of selectivity in the operation. Figure 10 shows a kaolinite

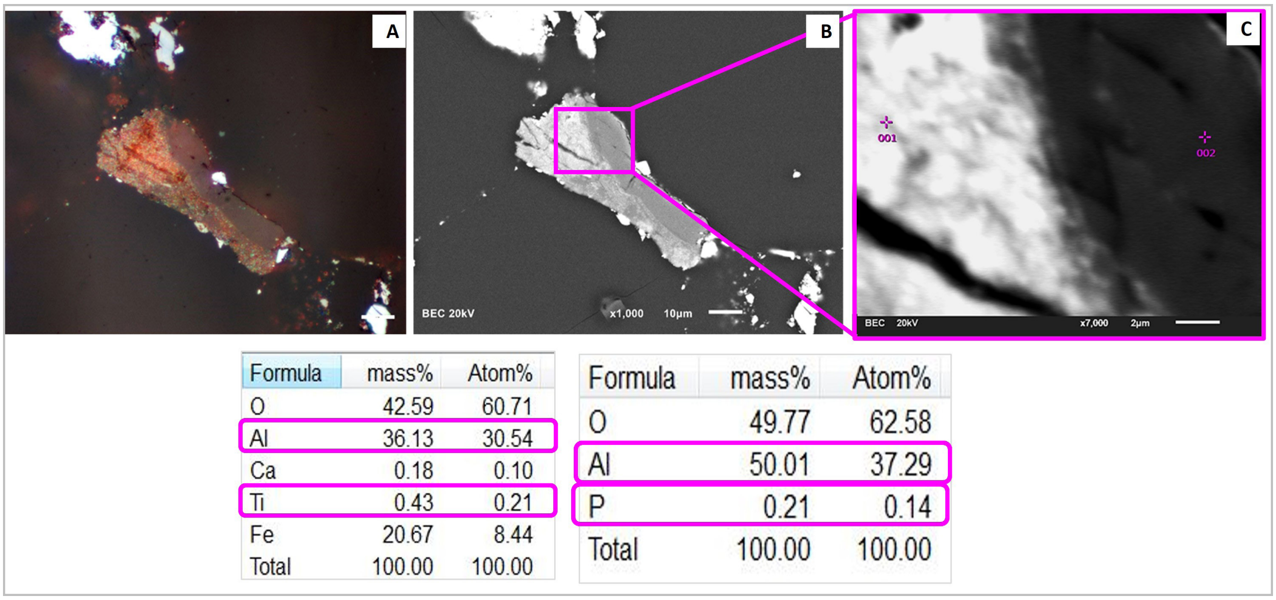

Formula	mass%	Atom%
O	42.59	60.71
Al	36.13	30.54
Ca	0.18	0.10
Ti	0.43	0.21
Fe	20.67	8.44
Total	100.00	100.00

Formula	mass%	Atom%
O	49.77	62.58
Al	50.01	37.29
P	0.21	0.14
Total	100.00	100.00

Figure 9. Micrographs of gibbsite particle by optical miroscopy (A) and SEM (B and C), showing evidence of phosphorus, with microprobe analyzes (below).

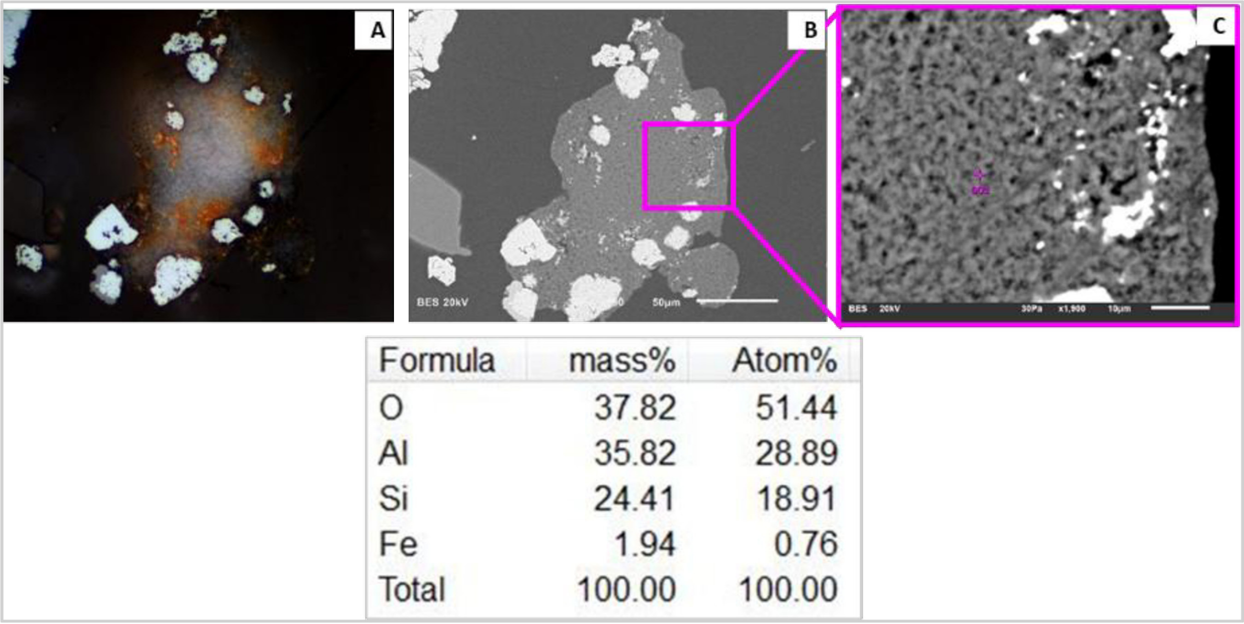

Formula	mass%	Atom%
O	37.82	51.44
Al	35.82	28.89
Si	24.41	18.91
Fe	1.94	0.76
Total	100.00	100.00

Figure 10. Micrographs of kaolinite by optical microscopy (A) and SEM (B and C) and microprobe analysis (below).

particle, which has appeared in larger contents in some of the samples (Table 1).

Figure 11 illustrates the occurrence of phosphorus associated with goethite, besides titanium in a silicate rich in aluminum. This observation supports the correlation already observed between phosphorus and goethite, as well as of aluminum and titanium.

Previous studies [12] have shown that one important target during mineral processing is to remove as much aluminum as possible. Besides the fact that it is present

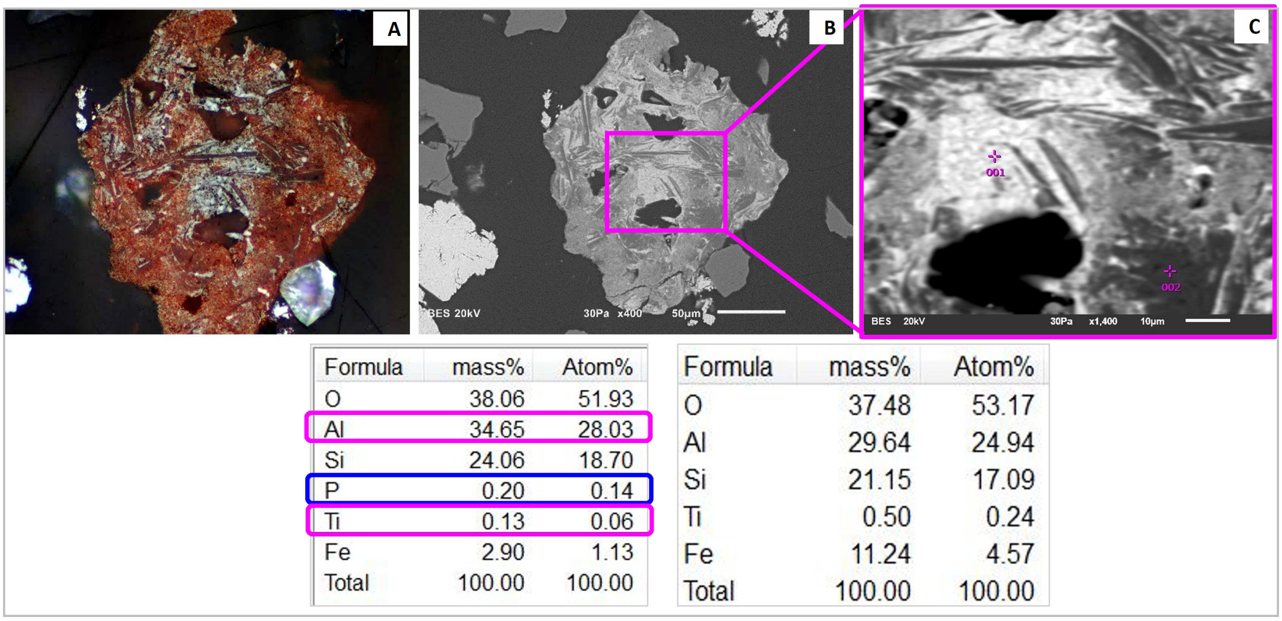

Formula	mass%	Atom%
O	38.06	51.93
Al	34.65	28.03
Si	24.06	18.70
P	0.20	0.14
Ti	0.13	0.06
Fe	2.90	1.13
Total	100.00	100.00

Formula	mass%	Atom%
O	37.48	53.17
Al	29.64	24.94
Si	21.15	17.09
Ti	0.50	0.24
Fe	11.24	4.57
Total	100.00	100.00

Figure 11. Micrograph of philosilicate by optical microscopy (A) and SEM (B and C) and microprobe analyzes (below).

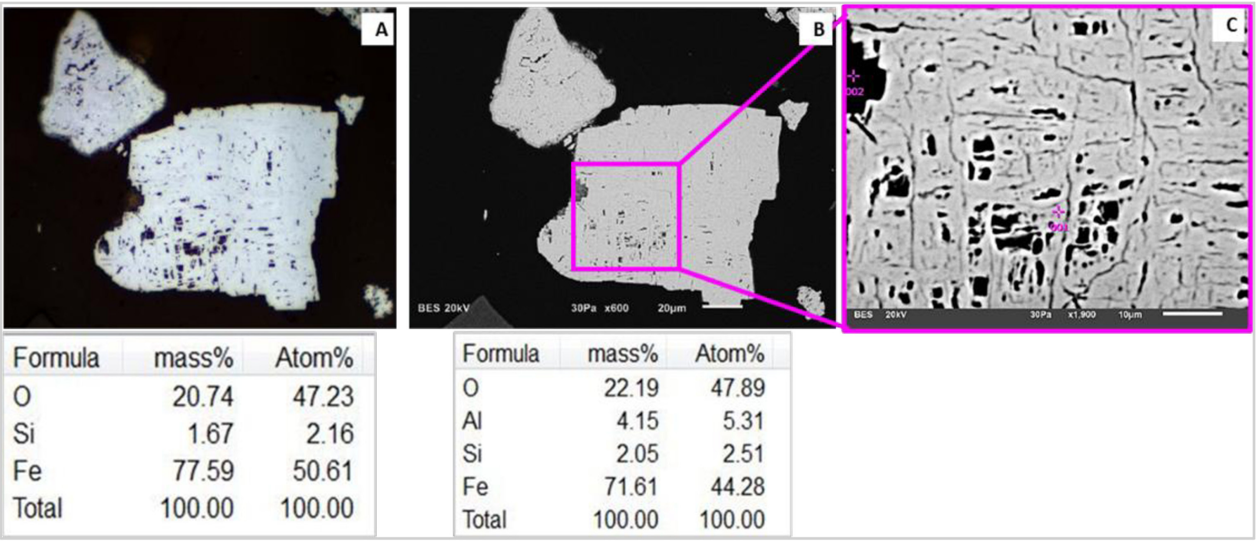

Formula	mass%	Atom%
O	20.74	47.23
Si	1.67	2.16
Fe	77.59	50.61
Total	100.00	100.00

Formula	mass%	Atom%
O	22.19	47.89
Al	4.15	5.31
Si	2.05	2.51
Fe	71.61	44.28
Total	100.00	100.00

Figure 12. Micrograph of martitic hematite by optical microscopy (A) and SEM (B and C) and microprobe analyzes (below).

in the form of aluminum oxides and hydroxides or in silicates, this metal may also isomorphically replace iron in the structure of hematite and goethite. Figure 12 shows a martitic hematite in which aluminum and silicium are dissolved in its structure, making its removal unfeasible, being carried to the concentrate and then to the iron ore pellet.

A greater challenge consists in removal of impurities contained in goethite. Figure 13 shows an earthy goethite particle that contains aluminum, silicium, phosphorus,

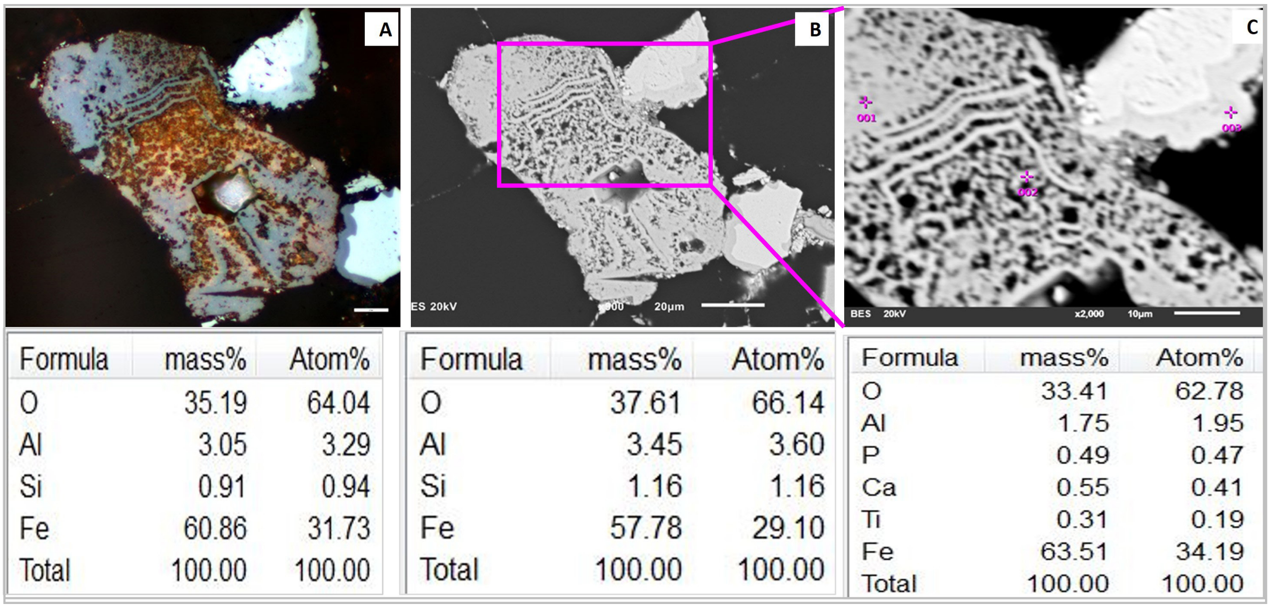

Formula	mass%	Atom%
O	35.19	64.04
Al	3.05	3.29
Si	0.91	0.94
Fe	60.86	31.73
Total	100.00	100.00

Formula	mass%	Atom%
O	37.61	66.14
Al	3.45	3.60
Si	1.16	1.16
Fe	57.78	29.10
Total	100.00	100.00

Formula	mass%	Atom%
O	33.41	62.78
Al	1.75	1.95
P	0.49	0.47
Ca	0.55	0.41
Ti	0.31	0.19
Fe	63.51	34.19
Total	100.00	100.00

Figure 13. Micrographs of earthy goethite in optical microscopy (A) and SEM (B and C) and microprobe analysis (below).

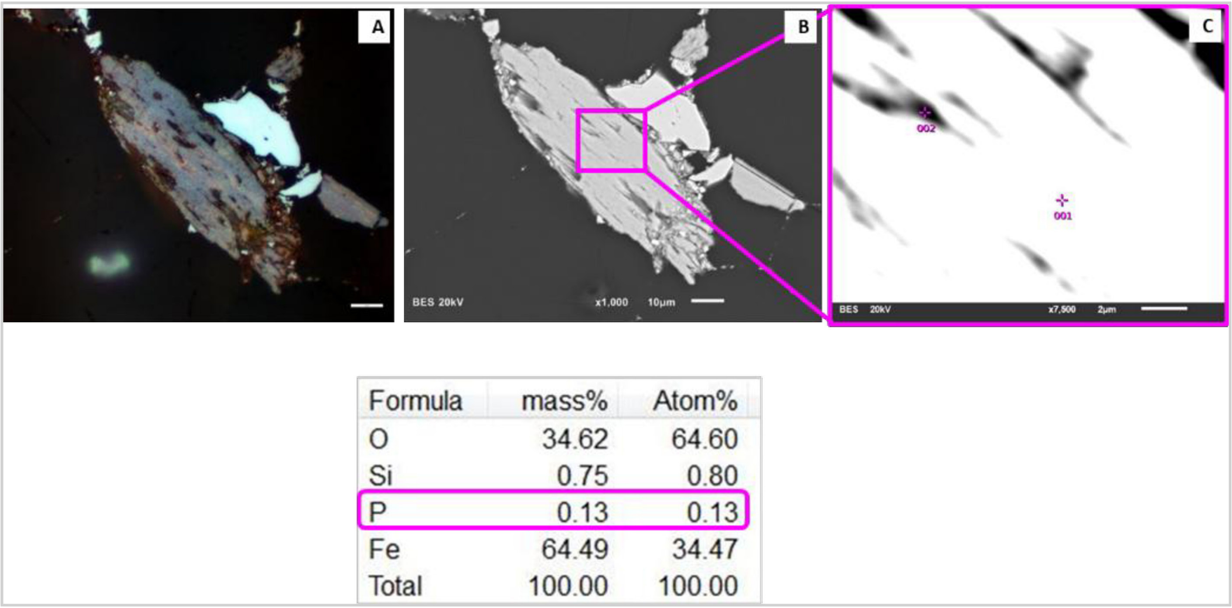

Formula	mass%	Atom%
O	34.62	64.60
Si	0.75	0.80
P	0.13	0.13
Fe	64.49	34.47
Total	100.00	100.00

Figure 14. Micrograph of pseudomorph goethite from amphibole from optical micrograph (A) and SEM (B and C) and microprobe analysis (below).

calcium and titanium as contaminants. These usually are carried along the concentrate into pelletization, affecting the chemical composition of the iron ore pellet.

Figure 14 shows a pseudomorphous goethite from amphibole. The mineral contains dissolved phosphorus in its structure, which probably will report to the concentrate and, therefore, to the final pellet.

Figure 15 shows a brotrioidal goethite, where mineral associations occur, with the phosphorus being present in different contents inside the structure of goethite.

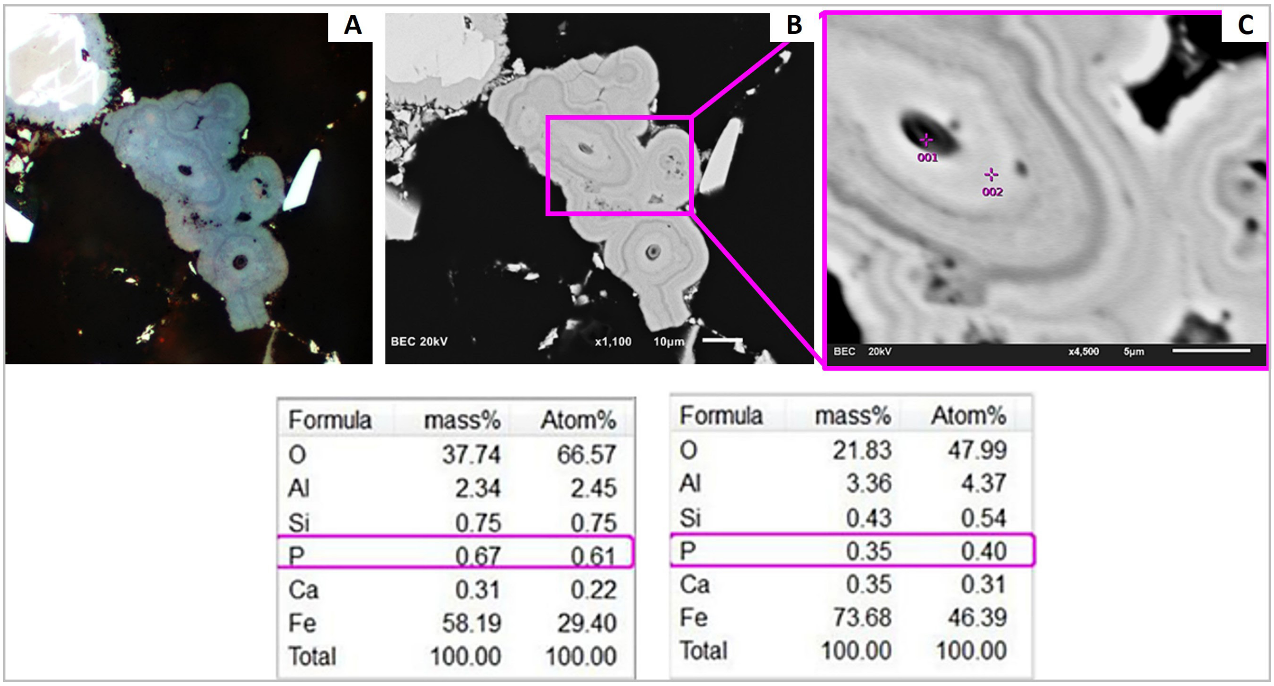

Formula	mass%	Atom%
O	37.74	66.57
Al	2.34	2.45
Si	0.75	0.75
P	0.67	0.61
Ca	0.31	0.22
Fe	58.19	29.40
Total	100.00	100.00

Formula	mass%	Atom%
O	21.83	47.99
Al	3.36	4.37
Si	0.43	0.54
P	0.35	0.40
Ca	0.35	0.31
Fe	73.68	46.39
Total	100.00	100.00

Figure 15. Micrographs of botrioidal goethite in optical microscopy (A) and SEM (B and C) and microprobe analyzes (below).

4 Conclusions

The different techniques used in characterizing the samples from the different mine faces from the Alegria complex provided elements to assess the ore tipologies with a focus on assessing the elements that pose challenges in the application of iron ore pellets in steelmaking.

The analysis of clay minerals, mineral associations with different degrees of liberation and the assessment of liberated, as well as binary and ternary locked particles showed that aluminum, in all samples is carried to the product mainly through goethite, kaolinite, micas and gibbsites. Phosphorous, on the other hand, is carried by the goethite and by the phosphates, in particular apatite. Manganese is mainly associated with Mn oxide-hydroxides, representing up to 5% in amphibolites. Titanium is mostly associated with ilmenite, besides titanium oxide, goethite and kaolinite. Correlations between goethite and phosphorous contents and with LOI, as well as between aluminum and titanium have been demonstrated to be high, showing that although goethite is the main source of contaminants in the ore, it is not the only source of phosphorous, aluminum and titanium, since these latter are also found in clay minerals, phyllosilicates and phosphates.

Acknowledgements

The authors would like to acknowledge the support from Samarco Mineração for this work.

References

1 Otaviano MM. Auto-fluxagem do fósforo em pelotas de redução direta [tese]. Rio de Janeiro: PUC-RIO; 2012.

2 Chemale FJ, Takehar AL. Minério de ferro: geologia e geometalurgia. São Paulo: Edgard Blucher; 2013.

3 Costa GM, Couto MLF, Carioca AC, Dutra FC. Formas de ocorrência de alumínio e fósforo em minérios de ferro. Tecnologia em Metalurgia e Materiais. 2010;6(4):206-209. https://doi.org/10.4322/tmm.00604004.

4 Ler A, Stanforth R. Evidence for surface precipitation of phosphate on goethite. Environmental Science & Technology. 2003;37(12):2694-2700. https://doi.org/10.1021/es020773i.

5 International Organization for Standardization. ISO 9516-1: determinação de vários elementos por espectrometria de fluorescência de raio-X. Geneva: ISO.

6 International Organization for Standardization. ISO 11536: determinação de perda por calcinação: método gravimétrico. Geneva: ISO.

7 International Organization for Standardization. ISO 2597-2: determinação do teor de ferro total – parte 2: métodos de titulação após redução por cloreto de titânio (III). Geneva: ISO.

8 Wills BA. Mineral processing technology: an introduction to the practical aspects of ore treatment and mineral recovery. 7th ed. Oxford: Elsevier; 2006.

9 Couto MLF. Caracterização de alumínio e fósforo em minério de ferro [dissertação]. Ouro Preto: Departamento de Engenharia de Minas, Universidade Federal de Ouro Preto; 2009.

10 Coelho LH, Fonseca L, Kaneko KM, Melo JC. A origem do fósforo e sua localização espacial nos minérios de ferro enriquecidos supergenicamente. In: Anais do II Simpósio Brasileiro de Minério de Ferro; 1999; Ouro Preto. São Paulo: ABM; 1999.

11 Rodrigues OMS. Investigação da cinética de flotação da Caulinita e do quartzo e sua implicação na Flotação reversa de minério de ferro. In: Anais do 64° Congresso Anual da ABM; 2009; Belo Horizonte. São Paulo: ABM; 2009.

12 Sis H, Chander S. Reagents used in the flotation of phosphate ores: a critical review. Minerals Engineering. 2003;16(7):577-585. https://doi.org/10.1016/S0892-6875(03)00131-6.

Received: 1 Nov. 2025
Accepted: 3 May 2026

Editor-in-charge:
André Carlos Silva